A discrete LQR applied to a self-balancing reaction wheel unicycle: Modeling, construction and control

Gabriel P. Neves[1] and Bruno A. Angélico[2].

***Abstract*— This work presents the modeling, construction and control of a self-balancing unicycle assisted by reaction wheel. It is a nonlinear, unstable and multivariable system. A useful model is presented, based on the Lagrangian mechanics. Construction steps are explicitly described and some implementation aspects, regarding the reaction wheel actuator limitation, are highlighted. A discrete-time LQR controller is validated in simulation and in practical tests with the real system.**

I. INTRODUCTION

Reaction wheel is a type of actuator widely used by spacecrafts and satellites for attitude control [1], [2], [3]. There are other applications that consider reaction wheels as an actuator, such as the reaction wheel inverted pendulum, stabilization and assistance for motorcycle [4], bipedal robot systems [5] and more recently the Cubli system [6].

Considering the operation point as the origin, the unicycle can be interpreted as two inverted pendulum, one for the roll and another for the pitch angle, since the system is decoupled at this point. The inverted pendulum is one of the most studied systems in Control Engineering, since it is an unstable and nonlinear system [7]. Some variations of the classical pendulum were proposed, such as the Furuta pendulum [8] and the reaction wheel pendulum [9].

The most common self-balancing robot is the two wheel systems [10], whose commercial variation became famous with the segway system [11], that is widely used for indoor locomotion in large environments, like big stores and shopping malls.

This work considers a variation of a self-balancing robot with a single wheel in contact with the ground and a reaction wheel to compensate for the lateral imbalance. There are few works in the literature considering practical control applications in systems like that. In [12] it is presented the dynamic model and a Sliding Mode Controller (SMC) is considered for roll angle control and a Linear Quadratic Regulator (LQR) for pitch angle control. The same robot is also considered in [13], but it applies a fuzzy SMC for the roll angle.

The same unicycle was considered in [14], where a continuous robust decoupled $\mathscr{H}_2$ control based on LMI (Linear Matrix Inequalities) was developed. However, unlike [14], this work will cover a discrete-time linear approach around the unstable equilibrium point.

The paper focuses on the system construction, emphasizing some practical aspects regarding the torque limitation of the actuators. The mechanical modeling is obtained using the Lagrangian formulation. The control system is a discrete-time Linear Quadratic Regulator (LQR). The work has the following organization: Section II shows, in detail, the construction of the robot. Section III describes the mechanical model based on the Lagrangian mechanics, while Section IV presents the control design. Simulation and practical results are presented in Section V and, finally, Section VI points out the main conclusions.

II. CONSTRUCTION

The unicycle is separated into three parts, the body, the reaction wheel, and the travel wheel in contact with the ground as shown in Figure 1.

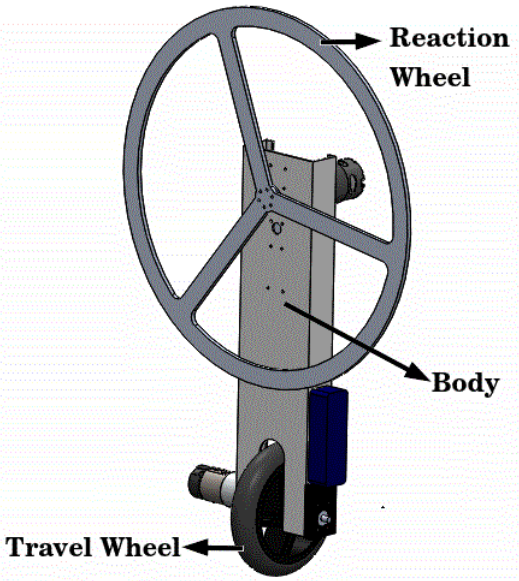

Fig. 1. Schematic drawing.

Firstly, the system was designed in 3D CAD software in order to dimension the actuators and to obtain the inertial parameters, as shown in Table I. The actuators are two DC gear-motor, with constants (K_{tr}, K_{er}, K_{tw}, K_{ew}) also presented in Table I. The real plant is presented in Figure 2.

The angular positions of both wheels are measured by incremental encoders, and their angular speeds are estimated

The authors would like to thank Fundação de Amparo à Pesquisa do Estado de São Paulo (FAPESP) (grants 2016/00729-9 and 2017/22130-4) and in part by the Coordenação de Aperfeiçoamento de Pessoal de Nível Superior - Brazil (CAPES) - Finance Codes 001 and 88882.333359/2019-01.

The authors are with Laboratory of Automation and Control, Dept. Telecommunications and Control Engineering, Escola Politécnica of the University of São Paulo (USP), Brazil

[1]gabriel.pereira.neves@usp.br

[2]angelico@lac.usp.br

TABLE I

PHYSICAL PARAMETERS.

	Parameter	Value
R_r	Reaction wheel radius [m]	0.2
R_w	Wheel radius [m]	0.071
L	Distance of the center of mass (CM) of the body [m]	0.18632
d	Distance between the CM of the body and reaction wheel [m]	0.1503
M_r	Reaction wheel mass [Kg]	0.47568
M_b	Body mass [Kg]	1.23913
M_w	Wheel mass [Kg]	0.30220
g	Acceleration of gravity [m/s^2]	9.8
J_r	Reaction wheel moment of inertia [kg m^2]	0.013472
J_w	Wheel moment of inertia [kg m^2]	0.00077
J_{br}	Moment of inertia of the body plus reaction wheel [kg m^2]	0.03937
J_{bw}	Moment of inertia of the body plus wheel [kg m^2]	0.03458
K_{tr}	Torque constant of the reaction wheel motor at the gearbox shaft [Nm/A]	0.3383
K_{er}	Electrical constant of the reaction wheel motor at the gearbox shaft [Vs^2/rad]	0.9454
R_{er}	Electrical resistance of the reaction wheel motor [Ω]	0.6
K_{tw}	Torque constant of the wheel motor at the gearbox shaft [Nm/A]	0.3531
K_{ew}	Electrical constant of the reaction wheel motor at the gearbox shaft [Vs^2/rad]	1.3465
R_{ew}	Electrical resistance of the wheel motor [Ω]	2.4
B_{vw}	Travel wheel viscous friction [Ns^2/rad]	0.1
B_{vr}	Reaction wheel viscous friction [Ns^2/rad]	0.1

using the Euler backward approximation with low pass filter. An inertial measurement unit (IMU), model GY-86, is used for measuring the pitch and the roll angular position and velocity. A Kalman filter is used to estimate the angular positions by fusing the gyroscope and accelerometer data, and their angular speeds are obtained directly from the gyroscope. Two H-bridges, model VNH2SP30, are used as DC motors drivers. The reaction wheel was built considering a 5mm aluminum plate with water jet cutting, and the unicycle body in an aluminum U profile with 2mm width.

All the components are on the body and the power is provided by a 3 cell LiPo battery, as observed in Figure 2. The control hardware, in which the control algorithm is embedded, is an NXP microcontroller, model FRDM-K64F, with the following main features: ARM Cortex M4 with 32-bit core, 120 MHz max clock frequency, 1024 KB program flash memory, 256 KB RAM.

An important point about the system construction is that it has a point of contact to the ground (convex wheel), unlike other works found in the literature that presents a line contact (flat wheel).

A. Reaction Wheel Torque Limitation

For guaranteeing the torque required for the reaction wheel to balance the system, a DC motor with gearbox was chosen. However, the dynamic torque during a complete motor reversion can damage the gearbox. The stall torque is given by 6 [Nm]. The worst case occurs when there is a reversal of direction, which can cause a very high dynamic torque, which would damage the gearbox. Therefore, a low-pass filter, presented in [14], will be used to avoid abrupt change of direction. This filter is define by

$$G_{lpf} = \frac{30}{s+30}. \tag{1}$$

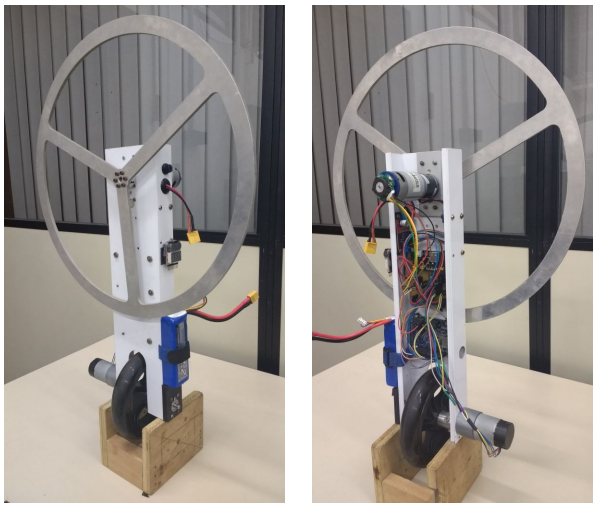

(a) View 1. (b) View 2.

Fig. 2. Practical unicycle

III. SYSTEM MODELING

The modeling is based in [14], however, this work will not take into account the uncertainties and the described approach of the linear model.

The unicycle robot has three parts, whose centers of mass (CMs) are determined by $\overrightarrow{p_1}$, $\overrightarrow{p_2}$ and $\overrightarrow{p_3}$, respectively, for the travel wheel, body and reaction wheel, as presented in Figure 3. These vectors are given by:

$$\overrightarrow{p_1} = \begin{bmatrix} R_w\theta_w & R_w\sin(\varphi) & R_w\cos(\varphi) \end{bmatrix}^\top, \tag{2}$$

$$\overrightarrow{p_2} = \begin{bmatrix} R_w\theta_w + L\sin(\psi) \\ (R_w + L\cos(\psi))\sin(\varphi) \\ (R_w + L\cos(\psi))\cos(\varphi) \end{bmatrix}, \tag{3}$$

$$\overrightarrow{p_3} = \begin{bmatrix} R_w\theta_w + (L+d)\sin(\psi) \\ (R_w + (L+d)\cos(\psi))\sin(\varphi) \\ (R_w + (L+d)\cos(\psi))\cos(\varphi) \end{bmatrix}, \tag{4}$$

where, θ_w, φ and ψ are the travel wheel angle, roll angle (around the x-axis) and pitch angle (around the y-axis), respectively.

A. Energy Calculation

Firstly, the translational kinetic energy is obtained as

$$E_T = \frac{1}{2}\overrightarrow{v}_i^\top M_i \overrightarrow{v}_i, \tag{5}$$

where M_i is the mass of the i-th body and $\overrightarrow{v}_i$ its velocity vector regarding the center of mass in relation to the inertial

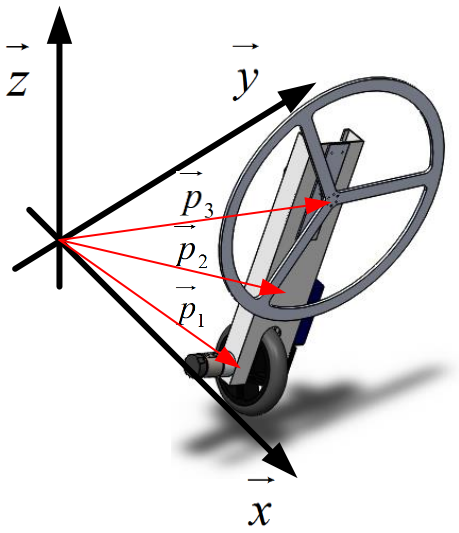

Fig. 3. CMs positions of unicycle robot.

frame. Considering the three parts of the unicycle, E_T is calculated as

$$E_T = \frac{1}{2}\vec{v_1}^\top M_w \vec{v_1} + \frac{1}{2}\vec{v_2}^\top M_b \vec{v_2} + \frac{1}{2}\vec{v_3}^\top M_r \vec{v_3}, \quad (6)$$

where,

$$\vec{v_1} = \frac{d}{dt}\vec{p_1}, \quad (7)$$

$$\vec{v_2} = \frac{d}{dt}\vec{p_2}, \quad (8)$$

$$\vec{v_3} = \frac{d}{dt}\vec{p_3}. \quad (9)$$

On the other hand, the rotational kinetic energy is obtained as

$$E_R = \underbrace{\frac{1}{2}J_w\dot{\theta}_w^2}_{1} + \underbrace{\frac{1}{2}J_{br}\dot{\psi}^2}_{2} + \underbrace{\frac{1}{2}J_r(\dot{\theta}_r+\dot{\varphi})^2}_{3} + \underbrace{\frac{1}{2}J_{bw}\dot{\varphi}^2}_{4}, \quad (10)$$

where parts 1 to 4 correspond, respectively, to the travel wheel rotation, the rotation of the pitch angle, the rotation of the reaction wheel and the rotation of the roll angle, and θ_r is the reaction wheel angle.

Assuming the ground as the reference frame, the height is given by the projection of $\vec{p_1}$, $\vec{p_2}$ and $\vec{p_3}$ on the $\vec{z}$ axis. The potential energy is then calculated as

$$\begin{aligned} U &= M_w g R_w \cos(\varphi) + M_b g((R_w + L\cos(\psi))\cos(\varphi)) + \\ &\quad M_r g(R_w + (L+d)\cos(\psi))\cos(\varphi). \end{aligned} \quad (11)$$

B. Lagrange Equation

The Lagrangian is defined as [15]

$$L = E_T + E_R - U. \quad (12)$$

Assuming that $q = \begin{bmatrix}\theta_r & \varphi & \theta_w & \psi\end{bmatrix}^\top$ is the vector of the generalized variables corresponding to the degrees of freedom and τ the vector of external torques and forces, the Lagrange equation can be written as

$$\frac{d}{dt}\frac{\partial L}{\partial \dot{q}} - \frac{\partial L}{\partial q} = \tau - B_v, \quad (13)$$

where $B_v = \begin{bmatrix}B_{vr}\theta_r & -B_{vr}\theta_r & B_{vw}\theta_w & -B_{vw}\theta_w\end{bmatrix}^\top$ is the vector of the viscous friction, with B_{vr} and B_{vw} being the terms regarding the reaction and travel wheel, respectively. The external torque is due to the motors and their reactions, such that

$$\tau = \begin{bmatrix}\tau_r & -\tau_r & \tau_w & -\tau_w\end{bmatrix}^\top, \quad (14)$$

where τ_r is regarding the reaction wheel motor and τ_w related to the travel wheel. The DC motors are modeled as

$$\tau_r = \frac{K_{tr}}{R_{er}}(12PWM_r - K_{er}\dot{\theta}_r), \quad (15)$$

$$\tau_w = \frac{K_{tw}}{R_{ew}}(12PWM_w - K_{ew}(\dot{\theta}_w - \dot{\psi})), \quad (16)$$

being, PWM_r and PWM_w the duty-cycle of PWM related to the reaction wheel and the travel wheel motors, which also include the direction of rotation, i.e., they are within $[-1, 1]$.

Since the objective of the paper is to balance the unicycle around its operation point, the states θ_r and θ_w can be eliminated from the model, because it is not desired to control them and they do not affect the other state variables. The state vector is then given by $x = \begin{bmatrix}\dot{\theta}_r & \varphi & \dot{\varphi} & \dot{\theta}_w & \psi & \dot{\psi}\end{bmatrix}$. Considering the origin as the operation point, the linear model is given by:

$$\dot{x}(t) = Ax(t) + Bu(t), \quad (17)$$

with matrices A and B being described as:

$$A = \begin{bmatrix}A_r & 0\\ 0 & A_w\end{bmatrix}, \quad (18)$$

$$B = \begin{bmatrix}B_r & 0\\ 0 & B_w\end{bmatrix}, \quad (19)$$

As can be seen, the linear model is decoupled, the states $\begin{bmatrix}\varphi & \dot{\varphi} & \dot{\theta}_r\end{bmatrix}$ do not interfere in $\begin{bmatrix}\psi & \dot{\psi} & \dot{\theta}_w\end{bmatrix}$, and vice versa. It is also valid for inputs τ_r and τ_w.

Substituting the values of Table I in Equations (18) and (19), it can be seen that:

$$A_r = \begin{bmatrix}-52.1139 & -21.9599 & 0\\ 0 & 0 & 1\\ 5.1226 & 21.9599 & 0\end{bmatrix}, \quad (20)$$

$$A_w = \begin{bmatrix}-67.5793 & -151.8787 & 44.9081\\ 0 & 0 & 1\\ 15.6751 & 58.3574 & -10.4165\end{bmatrix}, \quad (21)$$

$$B_r = \begin{bmatrix}557.0062\\ 0\\ -54.7512\end{bmatrix} \text{ and } B_w = \begin{bmatrix}400.2352\\ 0\\ -92.8352\end{bmatrix}. \quad (22)$$

The linear system was discretized considering zero-order hold and a sample time $Ts = 0.01s$, results in the following discrete-time system

$$x[n+1] = \Phi x[n] + \Gamma u[n], \quad (23)$$

where

$$\Phi = \begin{bmatrix} \Phi_r & 0 \\ 0 & \Phi_w \end{bmatrix}, \tag{24}$$

$$\Gamma = \begin{bmatrix} \Gamma_r & 0 \\ 0 & \Gamma_w \end{bmatrix}, \tag{25}$$

and

$$\Phi_r = \begin{bmatrix} 0.5938 & -0.1712 & -0.0009 \\ 0.0002 & 1.0011 & 0.0100 \\ 0.0399 & 0.2149 & 1.0011 \end{bmatrix}, \tag{26}$$

$$\Phi_w = \begin{bmatrix} 0.5305 & -1.0150 & 0.3062 \\ 0.0006 & 1.0025 & 0.0096 \\ 0.1090 & 0.4669 & 0.9301 \end{bmatrix}, \tag{27}$$

$$\Gamma_r = \begin{bmatrix} 4.3413 & -0.0023 & -0.4269 \end{bmatrix}^\top, \tag{28}$$

$$\Gamma_w = \begin{bmatrix} 2.7807 & -0.0036 & -0.6453 \end{bmatrix}^\top. \tag{29}$$

Note that the discrete system remains decoupled.

IV. DISCRETE TIME LQR CONTROL

The linear quadratic regulator (LQR) is an optimum control designed to minimize the following cost function in its discrete-time version [16]:

$$J = \sum_{k=0}^{\infty} x[k]^\top Q x[k] + u[k]^\top R u[k], \tag{30}$$

where Q and R are semi-definite positive matrices of state and control input weighting. The solution of this problem has a form of a simple state feedback

$$u[k] = -Kx[k], \tag{31}$$

being K given by [16]:

$$K = \left(R + \Gamma^\top P \Gamma\right)^{-1} \Gamma^\top P \Phi, \tag{32}$$

with P being the solution of the following discrete-time Algebraic Riccati Equation (ARE):

$$\Phi^\top \left(P - P\Gamma\left(R + \Gamma^\top P \Gamma\right)^{-1} \Gamma^\top P\right)\Phi + Q = P. \tag{33}$$

Bryson's rule can be considered for the first choice of Q and R [16]. It is a form of normalizing the state variables, where Q and R are diagonal matrices with elements,

$$Q_{ii} = \frac{1}{\text{maximum variation accepted of } x_i^2}, \tag{34}$$

and,

$$R_{jj} = \frac{1}{\text{maximum variation accepted of } u_j^2}. \tag{35}$$

Oftentimes it is just a starting point to a trial-and-error procedure. Bryson's rule was employed considering that the maximum angles of the system are approximately 15°, the maximum pitch and roll velocities are 10 [rad/s] and the maximum velocity of the motors are 118 [rpm]. It was also considered that the maximum variation of the PWM duty-cycle is 100% for both motors. The results LQR matrices are given by:

$$Q = \begin{bmatrix} 0.0065 & 0 & 0 & 0 & 0 & 0 \\ 0 & 14.5903 & 0 & 0 & 0 & 0 \\ 0 & 0 & 0.01 & 0 & 0 & 0 \\ 0 & 0 & 0 & 0.0065 & 0 & 0 \\ 0 & 0 & 0 & 0 & 14.5903 & 0 \\ 0 & 0 & 0 & 0 & 0 & 0.01 \end{bmatrix}, \tag{36}$$

and

$$R = \begin{bmatrix} 1 & 0 \\ 0 & 1 \end{bmatrix}. \tag{37}$$

With these choices, the control gain resulted in

$$K = \begin{bmatrix} -0.2819 & -14.5076 & -3.1595 & \dots \\ 0 & 0 & 0 & \dots \end{bmatrix} \tag{38}$$

$$\begin{matrix} \dots & 0 & 0 & 0 \\ \dots & -0.3410 & -9.3838 & -1.6206 \end{matrix}\Bigg], \tag{39}$$

Note that numbers with four decimal places were presented for the sake of space. For the simulation and practical application, the values are in double- and single-precision floating-point format, respectively.

V. SIMULATION AND PRACTICAL RESULTS

For simulations, the mechanical nonlinear model was considered, but strong nonlinearities, such as measurement noise, dead-zone of the actuators and backlash were not taken into account. Figure 4 shows this result. Initial condition of $-5°$ for φ and $5°$ for ψ were considered.

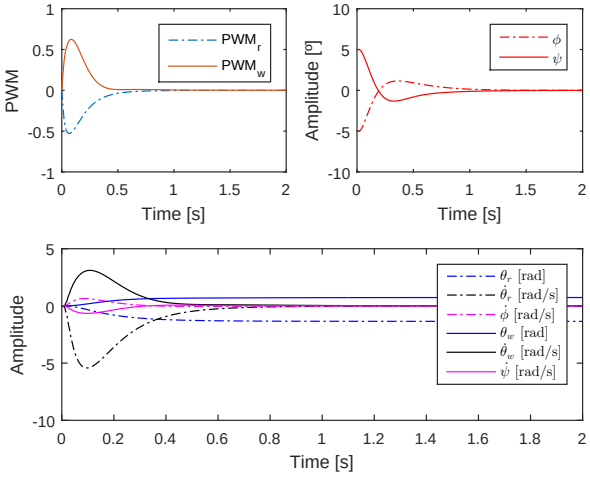

Fig. 4. Simulation of the discrete LQR.

The controller was able to stabilize the plant without saturating the actuators. One can note that θ_r and θ_w stabilize at non-zero points, which was expected because they were removed from the model used in the controller project. Figure 5 shows the control torque in each motor. As observed, their

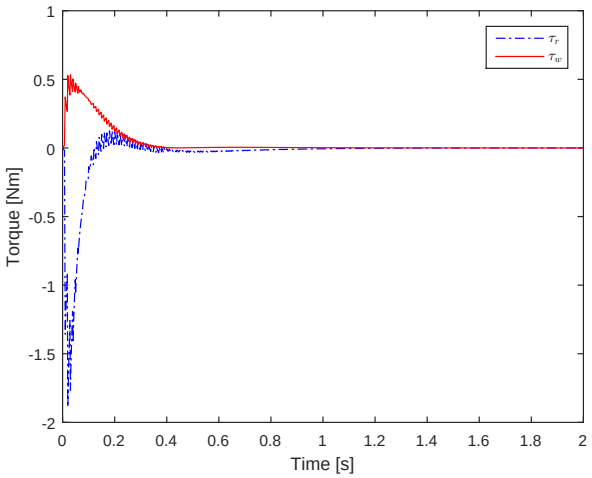

Fig. 5. Control effort (torque).

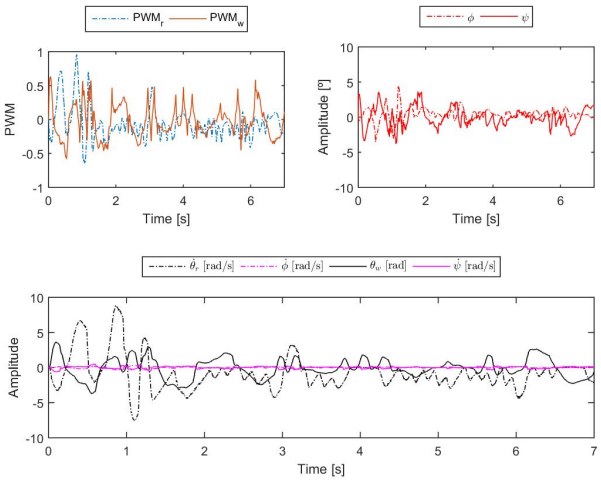

Fig. 6. Practical results of stabilization.

values remained much smaller than the stall torque of 6 [Nm].

Practical results with the built system are presented in Figure 6. As one can see, the controller was able to stabilize the robot with good performance.

Results considering an impulse (manual) disturbances applied in a diagonal way are presented in Figure 7. Again, the controller stabilized the system and was able to reject the disturbances.

A video of the robot working is available at the Youtube channel of the Laboratório de Controle Aplicado, Escola Politécnica of University of São Paulo, in the following link: `www.youtube.com/watch?v=t4sakACzcew`.

VI. CONCLUSIONS

A self-balancing unicycle with a reaction wheel was built, modeled and controlled in this work. A low pass filter was designed to limit the reaction wheel torque within a safe range for the gear-motor. The complete nonlinear model of

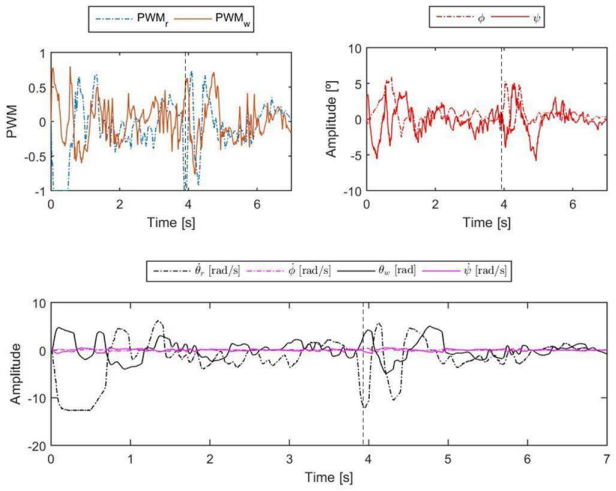

Fig. 7. Practical results of stabilization with diagonal disturbance rejection.

the robot is presented, based on the Lagrangian formulation. Linear Quadratic Regulator with weighting matrices derived from the Bryson's rule was designed and validated in simulation with the mechanical nonlinear model, and in practical tests, with the built system. The controller performed well in all tests. The system built is dynamically rich and can be considered as a practical test platform to more complex control techniques, like robust control, linear parameter varying control and nonlinear control methods.

REFERENCES

[1] M. C. Chou, C. M. Liaw, S. B. Chien, F. H. Shieh, J. R. Tsai, and H. C. Chang, "Robust current and torque controls for pmsm driven satellite reaction wheel," *IEEE Transactions on Aerospace and Electronic Systems*, vol. 47, no. 1, pp. 58–74, January 2011.

[2] M. de Athayde Costa e Silva, H. V. de Figueiredo, B. G. N. Boglietti, O. Saotome, E. Villani, and K. H. Kienitz, "A framework for development of satellite attitude control algorithms," *Journal of Control, Automation and Electrical Systems*, vol. 25, no. 6, pp. 657–667, Dec 2014. [Online]. Available: https://doi.org/10.1007/s40313-014-0141-7

[3] M. Aicardi, G. Cannata, and G. Casalino, "Smooth attitude feedback control with non-holonomic constraints," in *Proceedings of 35th IEEE Conference on Decision and Control*, vol. 2, Dec 1996, pp. 1706–1711 vol.2.

[4] A. Tanos, T. Steffen, and G. Mavros, "Improving lateral stability of a motorcycle via assistive control of a reaction wheel," in *Conference...* UKACC International Conference on Control, July 2014, pp. 80–85.

[5] T. L. Brown and J. P. Schmiedeler, "Reaction wheel actuation for improving planar biped walking efficiency," *IEEE Transactions on Robotics*, vol. 32, no. 5, pp. 1290–1297, Oct 2016.

[6] M. Muehlebach and R. D'Andrea, "Nonlinear analysis and control of a reaction-wheel-based 3-d inverted pendulum," *IEEE Transactions on Control Systems Technology*, vol. 25, no. 1, pp. 235–246, Jan 2017.

[7] F. H. D. Guaracy, R. L. Pereira, and C. F. de Paula, "Robust stabilization of inverted pendulum using alqr augmented by second-order sliding mode control," *Journal of Control, Automation and Electrical Systems*, vol. 28, no. 5, pp. 577–584, Oct 2017. [Online]. Available: https://doi.org/10.1007/s40313-017-0332-0

[8] K. Furuta, M. Yamakita, and S. Kobayashi, "Swing up control of inverted pendulum," in *Conference...* Industrial Electronics, Control and Instrumentation, Oct 1991, pp. 2193–2198 vol.3.

[9] F. Jepsen, A. Soborg, A. R. Pedersen, and Z. Yang, "Development and control of an inverted pendulum driven by a reaction wheel."

International Conference on Mechatronics and Automation, Aug 2009, pp. 2829–2834.

[10] S. Kim and S. Kwon, "Nonlinear optimal control design for underactuated two-wheeled inverted pendulum mobile platform," *IEEE/ASME Transactions on Mechatronics*, vol. 22, no. 6, pp. 2803–2808, Dec 2017.

[11] H. Bin, L. W. Zhen, and L. H. Feng, "The kinematics model of a two-wheeled self-balancing autonomous mobile robot and its simulation," in *Conference...*, vol. 2. Computer Engineering and Applications (ICCEA), March 2010, pp. 64–68.

[12] S. I. Han and J. M. Lee, "Balancing and velocity control of a unicycle robot based on the dynamic model," *IEEE Transactions on Industrial Electronics*, vol. 62, no. 1, pp. 405–413, Jan 2015.

[13] J. Lee, S. Han, and J. Lee, "Decoupled dynamic control for pitch and roll axes of the unicycle robot," *IEEE Transactions on Industrial Electronics*, vol. 60, no. 9, pp. 3814–3822, Sept 2013.

[14] G. P. Neves, B. A. Angélico, and C. M. Agulhari, "Robust $\mathscr{H}_2$ controller with parametric uncertainties applied to a reaction wheel unicycle," *International Journal of Control*, vol. 93, no. 10, pp. 2431–2441, 2020.

[15] J. J. Craig, *Introduction to Robotic: Mechanics and Control*, 3rd ed. Personal Education International, 2005.

[16] G. Franklin, J. Powell, and M. Workman, *Digital Control of Dynamic Systems*, 3rd ed. Ellis-Kagle Press, 2006.